Ziggurat Journal of Materials Technology (ZJMT)

(ISSN 2633-3155 online)

Journal Homepage: https://zigguratpublishing.com/index.php/zjmt

Article

Impact of PS/PMMA Polymer Ratios with Nanocomposite Material on Optical and Morphological Properties

Adawiya J. Haider [a, *], Zeyad Y. Al-Shibaany [b, c], Ryiam F. Hawy [d], Niheda J. Hamed [d]

[a] *Applied Science Department, Laser Branch, University of Technology - Iraq, Baghdad, 10066, Iraq.*
[b] *Biomedical Engineering Department, University of Technology - Iraq, Baghdad, 10066, Iraq.*
[c] *School of Engineering, Cardiff University, Cardiff CF24 3AA, UK.*
[d] *Applied Science Department, Material Branch, University of Technology - Iraq, Baghdad, 10066, Iraq.*
[*] *Corresponding author: 100081@uotechnology.edu.iq*
DOI: 10.36533/zjmt.v1i1.39

ARTICLE INFORMATION

Article History
Received: 10 August 2020
Revised: 25 September 2020
Accepted: 19 October 2020
Published: 11 November 2020

Keywords
PS
PMMA
Nanocomposite
TiO_2
Morphology
Optical properties
Rhodamine 6G

ABSTRACT

In this work, nanocomposite material consisting of titanium dioxide (TiO_2) nanoparticles and rhodamine 6G (R6G) laser dye was doped with different ratios of polystyrene (PS) and polymethylmethacrylate (PMMA) polymer blends (i.e. 40% PS/60% PMMA and 50% PS/50% PMMA) using the casting method. The optical properties of the prepared samples were measured using UV-visible spectroscopy. These measurements include the calculations of the absorption (A%), absorption coefficient (α), energy gap (Eg), refractive index (n), extinction coefficient (K) and real and imaginary parts. These nanocomposite materials were investigated using a scanning electron microscope and photoluminescence (PL) spectra emission. The SEM results show that the optimum results were at 50% PS/50% PMMA/TiO_2/R6G with all the dye being decorated in the process blend, while the TiO_2 nanoparticle demonstrated that the pores were incomplete in some places and complete in others. The optical results show that there are red shifts in all absorption peaks caused by the increased PS ratio. The Eg decreased from 3.2 eV to 2.8 eV as the concentration of PS in the polymer matrix increased. The PL spectrum for the nanocomposites, with a different ratio of PS, shows that sharp peaks of PL emission occur at a wavelength of 570 nm and shift towards longer wavelengths with an increased PS%.

1. Introduction

In the last few years, there has been a remarkable surge of interest in the development and preparation of solid-state organic-compound laser-active media that substitute for the liquid-compound media of tuneable lasers, thereby making their application more convenient and safer. Researchers have made significant progress due to recent advances in synthetic science [1]. Compared to a decade ago, researchers are now more attracted by both organic and inorganic nanocomposite materials because of their applicability to optoelectronic devices, such as solar cells, active media, photodiodes and organic light-emitting diodes [2]. Polymer nanocomposites have attracted considerable attention due to their unique properties and their numerous possible applications in modern technology [3-5]. Polymer-based nanocomposites have been developed that exhibit interesting optical properties, such as tailored absorption/emission. These composites are typically obtained through the incorporation of functional inorganic particles into suitable transparent polymer matrices. Various metal oxide fillers, such as ZnO, SiO_2, Al_2O_3 and TiO_2, have been incorporated into polymers to modify their overall optical properties [3]. TiO_2 materials are interesting due to their potential applications in optoelectronic devices [4, 5]. A

significant amount of research has focused on the development of TiO_2/polymer-blend nanocomposite material using different polymer systems. Introducing TiO_2 filler into polymeric matrices can modify the optical, electrical and mechanical properties [3, 6]. Polystyrene (PS) and polymethylmethacrylate (PMMA) are transparent thermoplastic materials [3, 4]. The PS/PMMA blend is a well-known immiscible combination for which bulk and surface phase separation has been observed [7-9]. Due to entropy mixing, polymeric blends are mostly incompatible and exist as a phase under appropriate conditions [10]. Recently, PS/PMMA blends based on micro/nanostructures located on a substrate/dye-doped polymer film/air waveguide structure have been widely investigated in random laser applications. This is used in many application fields, including medical, industrial and commercial. The proposed potential applications of random lasers are based on their simplicity, durability and low cost [11, 12], which makes them different to regular lasers.

In this work, PS/PMMA/TiO_2/R6G nanocomposites were prepared with different weight ratios of blends using the casting method to investigate their structural features and optical properties, using a scanning electron microscope (SEM), UV-visible spectroscopy and photoluminescence (PL), and to see how the choice of polymer blend in the nanocomposites influences the optical characteristics for future use as random laser active media. The rest of the paper is organised as follows. Section 2 explains the experimental work, which includes the materials, methods and the characterisation. The results and the discussion are illustrated in section 3. This is followed by the conclusion.

2. Experimental Work

2.1 Materials and Methods

The TiO_2 (with Mw = 79.865 g/mol), as nanoparticles, was supplied by SICMA. The R6G laser dye ($C_{28}H_{31}N_2O_3CL$ with Mw = 479.02 g/mol) was supplied by Lambda Physics LC (5900). The PMMA ($CH_2CH_3COOCH_3$ with Mw = 8400 g/mol), PS ((C_8H_8) n with Mw = 23700 g/mol) and dichloromethane (CH_2CL_2 with Mw = 84.93 g/mol) were supplied by ICI. Polymer solutions were prepared by dissolving the PS/PMMA in various weight ratios (40% PS/60% PMMA and 50% PS/50% PMMA) in methylene chloride. The solutions were mixed at room temperature and stirred for two hours. The concentrations of TiO_2 and R6G powder were 10^{-3} and were suspended in polymer-blend solutions and shaken in the magnetic stirrer for one hour until a pink-coloured solution was obtained. The solutions were then poured onto glass plates and methylene chloride was slowly evaporated overnight under ambient conditions. The nanocomposite materials were prepared using the casting method with a weight ratio of 4:3:3 (TiO_2:R6G:PS/PMMA blend).

2.2 Characterisation

The surface morphology of the samples was examined using the SEM analysis model TESCAN BRNO-Mira 3 LMU, made by a multinational company established through the merger of a Czech company, TESCAN, and a French company, ORSAY PHYSICS. The optical properties, such as the absorbance and transmittance spectra, were examined using a UV/160/Shimadzu spectrophotometer in the wavelength range of 200–700 nm and at a scanning speed of 1500 nm/min. From these spectra, the energy gap, absorption coefficient and all the optical constants, such as the refractive index and the real and imaginary dielectric constant parts, were calculated. At the same time, the PL properties were measured using the Shimadzu spectrofluorophotometer detector (RF-551) model.

3. Results and Discussion

In Figure 1, the SEM images depict the surface morphology of the PS/PMMA before and after the addition of the TiO_2 nanoparticles/R6G dye with different concentrations of PS. The particles have an almost uniform size with an average particle size of 42 nm and a spherical shape. Figures 1(b) and (c) show the SEM images of the 40% PS/60% PMMA and 50% PS/50% PMMA blends, respectively. The SEM images of the PS confirm the formation of plastic deformation and high porosity. The pores have different shapes and sizes that exhibit nano cracks caused by the temperature. The porosity of the sample increased as the PS ratio increased. The presence of microsized domains embedded in the PMMA matrix and larger, irregularly shaped domains interpenetrated in the PMMA phase can be clearly observed. In Figure 1(b), the surface of the blend reveals a high level of plastic deformation, which clearly shows that the adhesion between the PS and the PMMA is improved. These results are in agreement with [13, 14]. Figure 1(c) shows the incompatible immiscible behaviour of the blend, and the surface of the pure blend shows a plastic deformation or drawing. The holes are attributed to the porosity of the PS, and the results prove that the blend compatibility decreased as the PS ratio increased. Figures 1(d) and (e) show the surface morphology of the PS/PMMA/TiO_2/R6G nanocomposite. The films show many aggregations or chucks randomly distributed throughout the TiO_2 nanoparticles and R6G dye on their upper surface. These results are in agreement with [15-18]. Based on Figure 1(d), the results prove that the matrix surrounding the composite material

(PS/PMMA/TiO_2/R6G) developed microplastic deformation and became rough, but no deformation appeared. Many PS particles were dispersed in the matrix, and the particle size decreased. These results demonstrate the good adhesion capability of the 40% PS/60% PMMA blend. It was observed that the PS domain size decreased with the addition of TiO_2. Figure 1(e) shows less adhesion between the PMMA and PS than can be seen in Figure 1(d). It was observed that, for 50%PS/50% PMMA/TiO_2/R6G, all the dye was decorated in the process blend, while the TiO_2 nanoparticle demonstrates that the pores are incomplete in some places and complete in others.

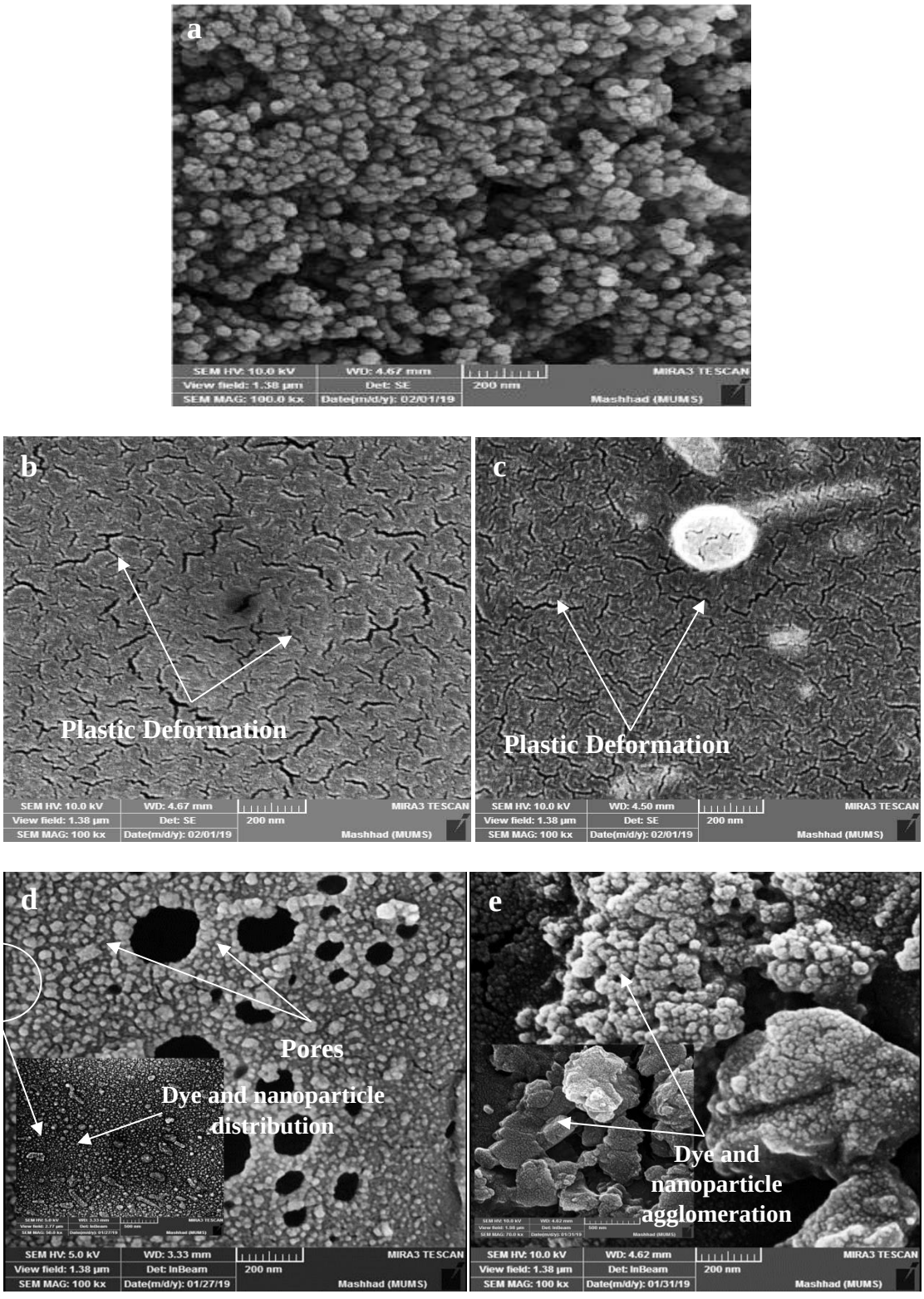

Fig. 1 - SEM images for the morphology of the films: (a) TiO_2 nanoparticle; (b) 40% PS/60% PMMA; (c) 50% PS/50% PMMA; (d) 40% PS/60% PMMA/TiO_2/R6G; (e) 50% PS/50% PMMA/TiO_2/R6G.

UV-visible studies were carried out in order to understand the transition at electronic levels in the prepared polymer nanocomposites (PNCs). Figure 2 illustrates the absorption spectra of the PS/PMMA blend at different concentrations and the RG6/TiO_2 NPs-doped PS/PMMA blend. From this it was possible to obtain the different types of electronic transitions, such as π–π* and n–π*. In the UV and visible regions, the absorption of light or photon energy of the polymeric material involves the σ, π and n-orbital. The transition involved in the ultraviolet region (i.e. 160–260 nm) can be attributed to the n → σ* transition and is called an electronic transition. The π → π* and n → π* transitions necessitate relatively low energy [19, 20] and therefore appear at higher wavelengths, as shown in Figure 2.

The absorption peaks that appeared at the higher wavelength region of around 300–700 nm for the blend and nanocomposite materials are related to the existence of the π-electrons. In the absorption spectra of the polymer blend and the nanocomposite, the existence of the two characteristic absorption bands are at around 320–550 nm for 40% PS/60% PMMA, 315–530 nm for 50% PS/50% PMMA, 320–550 nm at 40% PS/60% PMMA/TiO2/RG6 and 315–530 nm with 50% PS/50% PMMA/TiO2/R6G.

Table 1- Optical properties of the polymer blends and nanocomposites.

Blend and nanocomposite	Eg (ev) at 400 nm	A at 400 nm	n at 400 nm	K 10^{-4} at 400 nm	ε_r at 400 nm	ε_i 10^{-4} at 400 nm
40% PS/60% PMMA	3.2	16.96	2.19	5.4	4.83	23.75
50% PS/50% PMMA	3.2	23.03	2.39	7.33	5.74	35.15
40% PS/60% PMMA/TiO_2/R6G	2.9	34.91	2.11	1.08	5.53	3.56
50% PS/50% PMMA/TiO_2/R6G	2.8	59.51	2.6	2.2	6.78	9.03

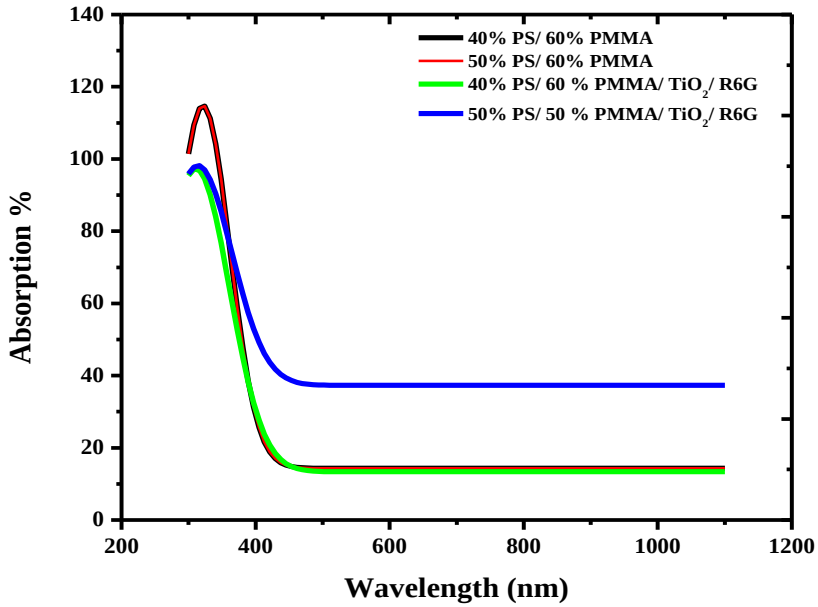

Fig. 2 - The absorption spectra of the different polymer blends and nanocomposites.

The peak absorption at different wavelengths ranging from 315 to 320 nm for different polymer blends and PNC films potentially arises from the π = π* (pi to pi star transition) electronic transition within the benzenoid segments. This result is in line with those of [20]. The second absorption at 530 and 550 nm for the different polymer blends and PNC films is related to the existence of π-electrons. The conjugated systems, consisting of alternating double bonds and single bonds, have been determined to be a centre of attraction among materials for the applications of optoelectronic devices because of their π-excessive nature [20]. The results reveal that there is a red shift for all samples. The shift is due to the change in the energy of the lowest unoccupied molecular orbital (LUMO) of the ligand that causes the π–π* and dπ–π* transitions to occur at a lower energy [21]. This result is in agreement with [22, 23].

The absorption coefficient (α) versus wavelength (λ) plot for the R6G/TiO_2-doped blend is shown in Figure 3. The result proves that there was a significant increase in the absorption coefficient with the addition of R6G/TiO_2. It

was found that the absorption coefficient spectra shifted towards longer wavelengths in comparison with the 40% PS/60% PMMA and 50% PS/50% PMMA blends, which is attributed to the R6G/TiO_2 NPs acting as localised states in the blend-energy gap [24].

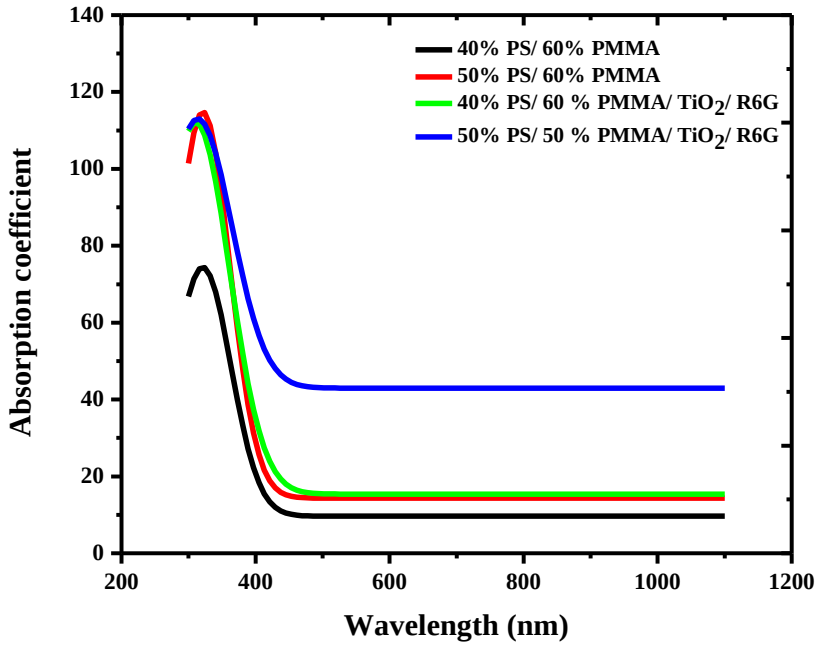

Fig. 3 - The absorption coefficient spectra of the samples with various concentrations of PS

Figure 4 shows the Eg of the R6G/TiO_2 NPs-doped blend. The energy-band gap was calculated by the mathematical treatment of the optical absorbance data using the Stern equation [1]:

$$(Ah\nu)^{2/n} = k'(k\nu - Eg) \quad (1)$$

where A is the absorbance, ν is the light constant in a unit of wavelength, h is Planck's constant, Eg is the energy band gap and k', k and n are constants. The Eg was obtained by extrapolating the straight line in a Tauc plot of $(Ahυ)^{2/n}$ as the function of hν to the base line, where $(Ahυ)^{2/n} = 0$. The optical energy-band gap of the R6G/TiO_2 doped with the PNCs decreased significantly in comparison with the blend. These results agree with [16, 24].

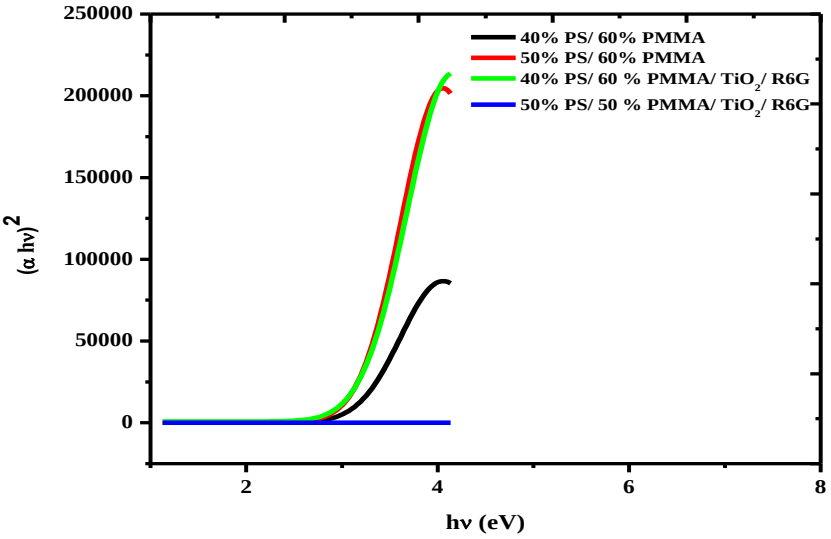

Fig. 4 - The energy-gap spectra of the samples with various concentrations of PS

Figure 5 shows the change in the reflective ion (R) with the wavelength (λ) due to interactions between the photons and electrons when n changes the λ of the light beam created by these reaction changes.

The value of n for a blend with R6G/TiO_2 increased. This rise in value is attributed to the R6G/TiO_2 acting at a local level in a similar way to the levels of impurities that lead to a rise in the Fermi level [25].

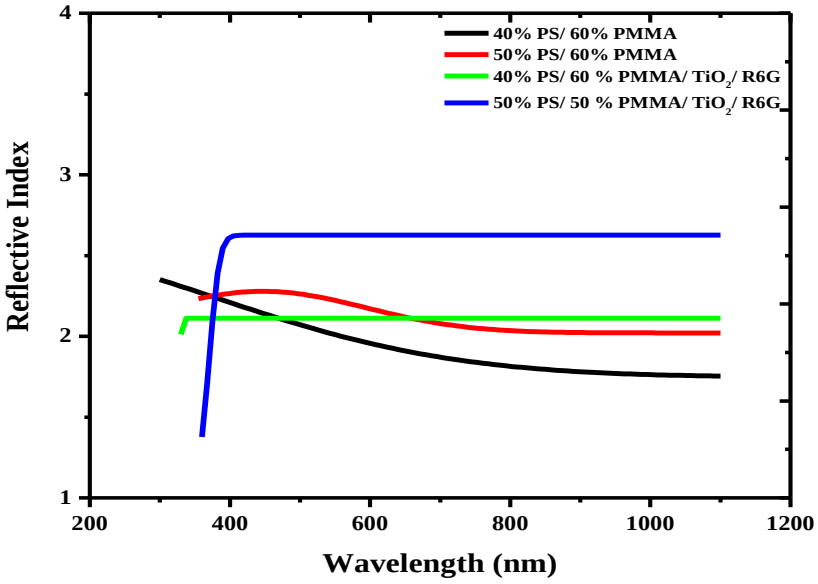

Fig. 5 - The reflective index spectra of the samples with various concentrations of PS

Figure 6 refers to the extinction coefficient (k) for the PNCs. The k value increased in comparison with the blend for the same reason [24].

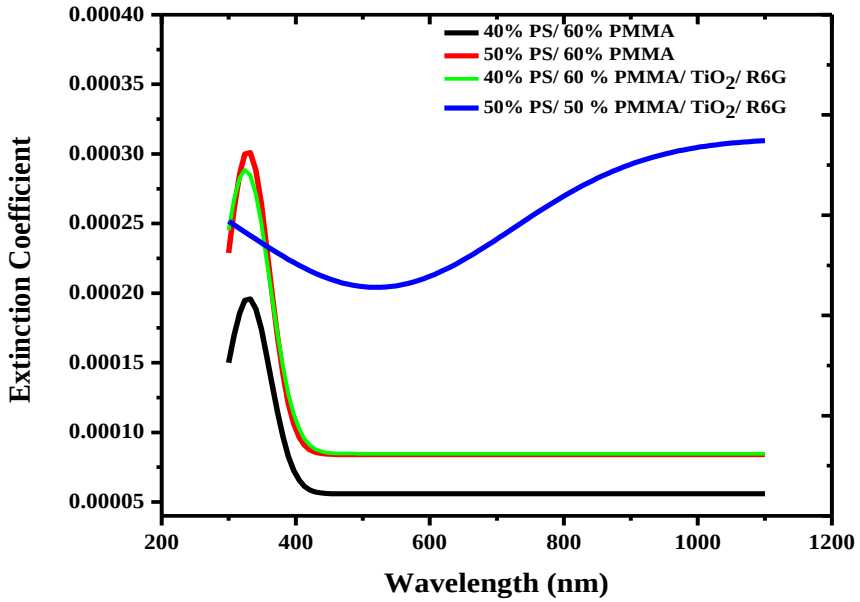

Fig. 6 - The extinction coefficient of the samples with various concentrations of PS.

The real dielectric constant part ε_r and the imaginary dielectric constant part ε_i are shown in Figures 7 and 8. As they relate to the n and k values, the ε_r and ε_i values were calculated [25]:

$$\varepsilon r = n2 - k2 \quad (2)$$

$$\varepsilon i = 2nk \quad (3)$$

In the real and imaginary parts of the dielectric constant for the dye/TiO_2-doped blend, the real part is associated with how much it slows down the speed of light in the material, and the imaginary part is associated with how a dielectric absorbs energy from the electric field due to dipole motion. The values of εr and εi significantly increased for the PNCs in comparison with the blend, which is attributed to the dye, and TiO_2 NP caused an increase in the free charge carriers in the blend [25].

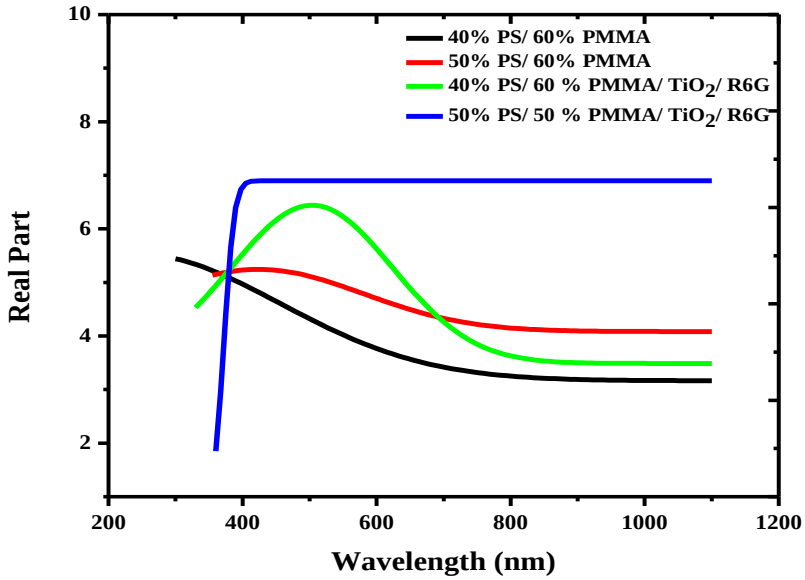

Fig. 7 - The real-part spectra of the samples with various concentrations of PS

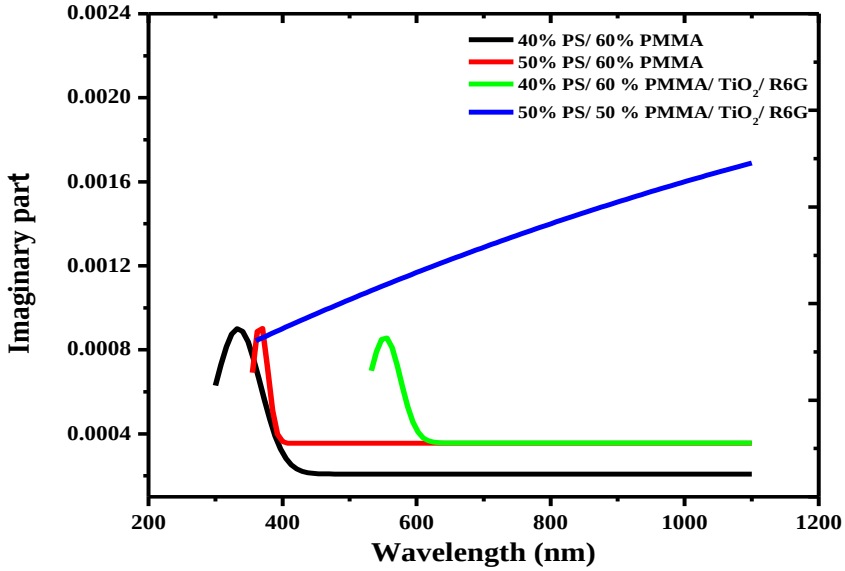

Fig. 8 - The imaginary-part spectra of the samples with various concentrations of PS

The various optical properties obtained for the composite materials for different cases are listed in Table 2.

Table 2 - Optical properties of the polymer blends and nanocomposites.

Blend and nanocomposite	Eg (ev) at 400 nm	A at 400 nm	n at 400 nm	K 10^{-4} at 400 nm	ε_r at 400 nm	ε_i 10^{-4} at 400 nm
40% PS/60% PMMA	3.2	16.96	2.19	5.4	4.83	23.75
50% PS/50% PMMA	3.2	23.03	2.39	7.33	5.74	35.15
40% PS/60% PMMA/TiO_2/R6G	2.9	34.91	2.11	1.08	5.53	3.56
50% PS/50% PMMA/TiO_2/R6G	2.8	59.51	2.6	2.2	6.78	9.03

The presence of R6G and TiO_2 NP thus enhanced the UV absorption of the composite films and modified the overall optical behaviour of the polymer-blend films. The PL spectra emission was measured at the wavelength range of 300–700 nm, which became excited at the pumping wavelength of 280 nm, as illustrated in Figure 9, which shows the PL spectra emission of the PS/PMMA/TiO_2/R6G nanocomposite with different concentrations of PS. Furthermore, the figure shows sharp peaks of PL emission occurring at a wavelength of 570 nm and shifting towards longer wavelengths (i.e. red shift) with an increase of PS%. It is also noteworthy that the emission intensity of the PL spectra at the ratio of PS:50% is much higher than at the ratio of 40%. These results agree with those of the shift in the UV-visible spectra. These shifts in bands to the visible region may be due to the interaction between PS/PMMA/TiO_2 and the R6G dye, which can be attributed to the inductive effect of the substituted groups in R6G, such as CH_3CH_2NH, $NHCH_2CH_3$, CH_3, Cl^- and CH_3CH_2O-C=O. This chromophoric group intensified and shifted the n–π* transition to the higher wavelength region, which is in agreement with the results of [2].

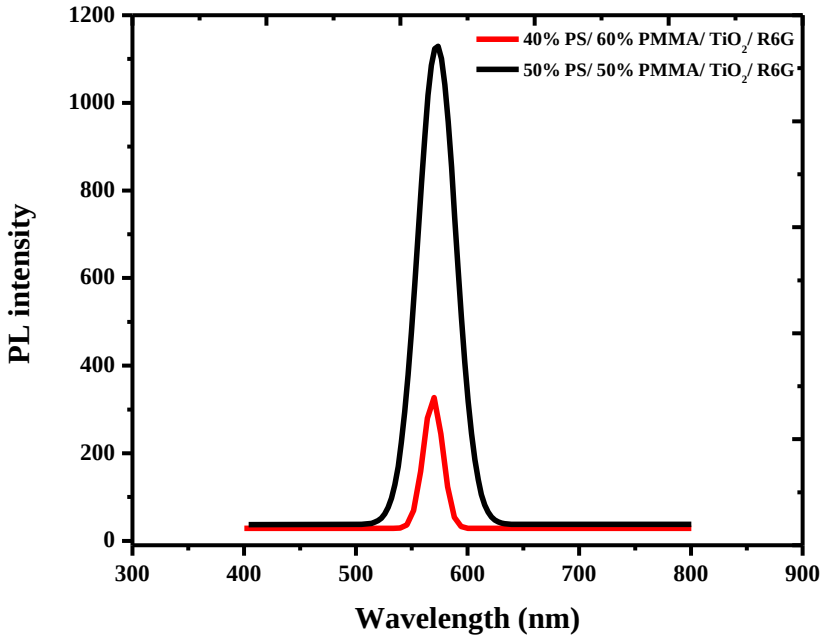

Fig. 9 - The PL emission spectrum of PS/PMMA/TiO_2/R6G of the samples with various concentrations of PS.

4. Conclusion

Different concentrations of the polymer blend and the PS/PMMA/TiO_2/R6G nanocomposite were successfully synthesised using the casting method. The optimum results were at 50% PS/50% PMMA/TiO2/R6G, where all the dye was decorated in the process blend. SEM studies clearly show the non-uniformity of distribution among particles with a polymer blend. The UV-visible spectra and PL emission confirm that there is a strong interaction between polymer blends and nanoparticles, which causes the red shift because the plasmon band shifts toward a higher wavelength (a red shift) with increasing TiO_2-particle size, and its quantum effect.

References

[1] T. N. Kopylova, V. B. Sukhanov, G. V. Mayer, A. V. Reznichenko, M. S. Dolotov, and A. A. Shaposhnikov, "Solid-state active media of tunable organic- compound lasers pumped with a laser. II. A copper vapor laser," *Applied Physics B,* vol. 74, no. 6, pp. 545-547, 2002/04/01 2002.

[2] M. Nandimath, R. F. Bhajantri, J. Naik, and V. Hebbar, "Effect of Rhodamine 6G dye on chromaticity co-ordinates and photoluminescence properties of TiO2/PMMA polymer nanocomposites for LED applications," *Journal of Luminescence,* vol. 207, pp. 571-584, 2019/03/01/ 2019.

[3] Y. Al-Douri, A. J. Haider, A. H. Reshak, A. Bouhemadou, and M. Ameri, "Structural investigations through cobalt effect on ZnO nanostructures," *Optik,* vol. 127, no. 20, pp. 10102-10107, 2016/10/01/ 2016.

[4] A. J. Haider, F. I. Sultan, and A. Al-Nafiey, "Controlled growth of different shapes for ZnO by hydrothermal technique," *AIP Conference Proceedings,* vol. 1968, no. 1, p. 030085, 2018.

[5] A. J. Haider and F. I. Sultan, "Structural, Morphological and Random Laser Action for Dye-ZnO Nanoparticles in Polymer Films."

[6] R. Palomino-Merino, J. Torres-Kauffman, R. Lozada-Morales, O. Portillo-Moreno, M. García-Rocha, and O. Zelaya-Angel, "Photoluminescence of Rhodamine 6G-doped amorphous TiO2 thin films grown by sol–gel," *Vacuum,* vol. 81, no. 11, pp. 1480-1483, 2007/08/28/ 2007.

[7] S. Walheim, M. Böltau, J. Mlynek, G. Krausch, and U. Steiner, "Structure Formation via Polymer Demixing in Spin-Cast Films," *Macromolecules,* vol. 30, no. 17, pp. 4995-5003, 1997/08/01 1997.

[8] J. J. Schmidt, J. A. Gardella Jr, and L. Salvati Jr, "Surface studies of polymer blends. 2. An ESCA and IR study of poly (methyl methacrylate)/poly (vinyl chloride) homopolymer blends," *Macromolecules,* vol. 22, no. 12, pp. 4489-4495, 1989.

[9] B. Jaleh, M. S. Madad, S. Habibi, P. Wanichapichart, and M. F. Tabrizi, "Evaluation of physico-chemical properties of plasma treated PS–TiO2 nanocomposite film," *Surface and Coatings Technology,* vol. 206, no. 5, pp. 947-950, 2011/11/25/ 2011.

[10] G. Krausch, "Surface induced self assembly in thin polymer films," *Materials Science and Engineering: R: Reports,* vol. 14, no. 1, pp. v-94, 1995/03/01/ 1995.

[11] R. Balachandran, D. Pacheco, and N. Lawandy, "Laser action in polymeric gain media containing scattering particles," *Applied optics,* vol. 35, no. 4, pp. 640-643, 1996.

[12] J. Dubois and S. La Rochelle, "Active cooperative tuned identification friend or foe (ACTIFF)," ed: Google Patents, 1999.

[13] L. Yang, S. Zhou, and L. Wu, "Preparation of waterborne self-cleaning nanocomposite coatings based on TiO2/PMMA latex," *Progress in Organic Coatings,* vol. 85, pp. 208-215, 2015/08/01/ 2015.

[14] N. Wang, N. Gao, Q. Fang, and E. Chen, "Compatibilizing effect of mesoporous fillers on the mechanical properties and morphology of polypropylene and polystyrene blend," *Materials & Design,* vol. 32, no. 3, pp. 1222-1228, 2011/03/01/ 2011.

[15] A. M. Nuruzatulifah, A. A. Nizam, and N. M. N. Ain, "Synthesis and Characterization of Polystyrene Nanoparticles with Covalently Attached Fluorescent Dye," *Materials Today: Proceedings,* vol. 3, pp. S112-S119, 2016/01/01/ 2016.

[16] S. Ningaraju, A. P. Gnana Prakash, and H. B. Ravikumar, "Studies on free volume controlled electrical properties of PVA/NiO and PVA/TiO2 polymer nanocomposites," *Solid State Ionics,* vol. 320, pp. 132-147, 2018/07/01/ 2018.

[17] L. Zan, L. Tian, Z. Liu, and Z. Peng, "A new polystyrene–TiO2 nanocomposite film and its photocatalytic degradation," *Applied Catalysis A: General,* vol. 264, no. 2, pp. 237-242, 2004/06/25/ 2004.

[18] A. Laachachi, M. Ferriol, M. Cochez, D. Ruch, and J. M. Lopez-Cuesta, "The catalytic role of oxide in the thermooxidative degradation of poly(methyl methacrylate)–TiO2 nanocomposites," *Polymer Degradation and Stability,* vol. 93, no. 6, pp. 1131-1137, 2008/06/01/ 2008.

[19] M. Hammam, M. K. El-Mansy, S. M. El-Bashir, and M. G. El-Shaarawy, "Performance evaluation of thin-film solar concentrators for greenhouse applications," *Desalination,* vol. 209, no. 1, pp. 244-250, 2007/04/30/ 2007.

[20] N. J. Hameed, A. J. Haider, and R. E. Hawy, "Optical properties study for PS/PMMA blend as laser active medium," *AIP Conference Proceedings,* vol. 2123, no. 1, p. 020022, 2019.

[21] A. J. Haider, F. I. Sultan, M. J. Haider, and N. M. Hadi, "Spectroscopic and structural properties of zinc oxide nanosphere as random laser medium," *Applied Physics A,* vol. 125, no. 4, p. 260, 2019/03/19 2019.

[22] E. S. Džunuzović, J. V. Džunuzović, A. D. Marinković, M. T. Marinović-Cincović, K. B. Jeremić, and J. M. Nedeljković, "Influence of surface modified TiO2 nanoparticles by gallates on the properties of PMMA/TiO2 nanocomposites," *European Polymer Journal,* vol. 48, no. 8, pp. 1385-1393, 2012/08/01/ 2012.

[23] A. M. Al-Baradi, S. F. Al-Shehri, A. Badawi, A. Merazga, and A. A. Atta, "A study of optical, mechanical and electrical properties of poly(methacrylic acid)/TiO2 nanocomposite," *Results in Physics,* vol. 9, pp. 879-885, 2018/06/01/ 2018.

[24] K. M. Ali, "Study of dyes effect in optical and Electrical Properties of Polystyrene (PS)," University of Technology - Iraq, 2013.

[25] M. H. Abdul-Allah, "Study of optical properties of (PMMA) doped by methyl red and methyl blue films," *Iraqi Journal of Physics (IJP),* vol. 12, no. 24, pp. 47-51, 2014.